NREL National Renewable Energy Laboratory

Innovation for Our Energy Future

Damp-Heat Induced Degradation of Transparent Conducting Oxides for Thin-Film Solar Cells

Preprint

F.J. Pern, R. Noufi, X. Li, C. DeHart, and B. To
National Renewable Energy Laboratory

NOTICE

Damp-Heat Induced Degradation of Transparent Conducting Oxides
for Thin-Film Solar Cells

F.J. Pern, R. Noufi[1], X. Li, C. DeHart, and B. To

National Center for Photovoltaics, National Renewable Energy Laboratory, 1617 Cole Blvd., Golden, CO 80401
[1] currently with SoloPower Inc., 5981 Optical Court, San Jose, CA 95138

ABSTRACT

The stability of intrinsic and Al-doped single- and bi-layer ZnO for thin-film CuInGaSe$_2$ solar cells, along with Al-doped Zn$_{1-x}$Mg$_x$O alloy and Sn-doped In$_2$O$_3$ (ITO) and F-doped SnO$_2$, was evaluated by direct exposure to damp heat (DH) at 85°C and 85% relative humidity. The results show that the DH-induced degradation rates followed the order of Al-doped ZnO and Zn$_{1-x}$Mg$_x$O >> ITO > F:SnO$_2$. The degradation rates of Al:ZnO were slower for films of higher thickness, higher substrate temperature in sputter-deposition, and with dry-out intervals. As inferred from the optical micro-imaging showing the initiation and propagation of degrading patterns and regions, the degradation behavior appears similar for all TCOs, despite the obvious difference in the degradation rate. A degradation mechanism is proposed to explain the temporal process involving thermal hydrolysis.

INTRODUCTION

Long-term performance reliability is required for all photovoltaic (PV) modules ranging from crystalline-Si based to thin films including CuInGaSe$_2$ (CIGS), CdTe, amorphous Si, dye-sensitized, and organic PV that employ transparent conducting oxides (TCOs) as electrical contacts or electrodes. Achieving this goal requires not only reliable constituent component materials and device structure of the solar cells, but also reliable electrical interconnects and packaging. To assess the quality of a PV module, one of the qualification tests in the IEC61215 or IEC61464 specifies a 1000-h exposure in damp heat (DH) at 85°C and 85% relative humidity (RH). Most CIGS solar cells use a combination of intrinsic and Al-doped ZnO as the conducting buffer layer. Reliability of the bi-layer i-/Al:ZnO (BZO), along with the Mo base electrode, can be the determining factor for durable long-term performance of a CIGS-based device/module. Similar reliability requirements of TCO-based contacts or electrodes are also applicable to other thin-film PVs.

In a previous paper, we reported some results from an exploratory study that demonstrated the instability of Mo and BZO when exposed to DH or to a 2.5 UV-sun at 60°C and 60% RH in a weatherometer (WOM) chamber [1]. The Mo was sputtered on 2.2-mm-thick soda lime glass. We found that Mo was rapidly corroded by the hot steam in DH condition, but was significantly less sensitive to the exposure in WOM and even less to the heating at 85°C in ambient relative humidity typically in the 11%~15% RH range in our laboratory. The BZO samples in that study were old "witness" films deposited along with CIGS solar cells on thin 0.5-mm 7059 glass slides with some variations in film quality. Nonetheless, when exposed to the DH, the "witness" BZO films were all degraded by the hot steam, but more rapidly in the presence of acetic acid vapor [1]. The acetic acid was intentionally introduced to simulate the possible presence of the acid from thermal processing and photothermal degradation of the ethylene-vinyl acetate (EVA) encapsulant commonly used in PV module encapsulation [2]. There are also some other studies on the stability issues of Al:ZnO by DH exposure reported in the literature [3-5].

In the present work, we used 1.1-mm-thick 7059 glass slides with single-layer intrinsic and Al-doped ZnO and bilayer i-/Al:ZnO that were specifically prepared with greater consistency in quality and property according to the "standard" conditions well established in our laboratory. The investigation was also extended to include Al-doped Zn$_{1-x}$Mg$_x$O alloy, Sn-doped In$_2$O$_3$ (ITO), and F-doped SnO$_2$ that can be employed as electrodes for various thin film solar cells. The Al-doped Zn$_{1-x}$Mg$_x$O alloy, fabricated in house, was tested to evaluate its potential to replace the conventional Al:ZnO. The present study focused only on the DH exposure-induced degradations. It should be emphasized that the direct exposure of the TCO coatings on the glass substrates to the DH conditions represents a fairly extreme situation that normally may not be experienced by a well-encapsulated and packaged PV module. This study, therefore, represents primarily our efforts to evaluate and compare the stability of various TCO materials for thin-film PV applications.

EXPERIMENTAL

To differentiate the differences among the three, 0.1-µm single-layer intrinsic ZnO and Al-doped ZnO, and 0.2-µm bi-layer ZnO were prepared separately by magnetron sputtering on 7.6-cm x 7.6-cm x 1.1-mm 7059 glass plates using a Semicore system, in which the *in-situ* substrate temperatures were determined to not exceed 60°C with a temperature indicator strip. Another set of single-layer Al-doped ZnO with or without MgO (Al:Zn$_{1-x}$Mg$_x$O, x= 0 to 0.1) at a thickness of 0.3~0.6 µm was made in an ATC 2200-V sputtering system from AJA International, Inc. The ambient substrate temperature inside the ATC system has

not yet been definitely determined. The ITO glass plates were previously provided by Applied Film Laboratory (AFL). One of the F-doped SnO_2 samples was made in house (ID# L6A3) and the other two were from glass manufacturers, one is a commercial product noted as P-TCE and the other is an experimental product noted as P-TCO. Specimens of ~2.0-cm x 2.8-cm were cut from the TCO-coated plates for exposures in a chamber operated at $85^{o}C$ and 85% RH. After baseline measurements, the TCOs were characterized periodically during the course of DH exposure by transmittance and reflectance measurements for optical properties, Hall measurements for sheet resistance, majority carrier mobility and concentration, x-ray diffraction (XRD) analysis for structural changes, and interference optical micro-imaging for morphological changes. Upon completion of the experiments, the exposed samples were examined with scanning electron microscopy (SEM). The systems used were a Cary 5G UV-Vis-NIR spectrophotometer with an integration sphere, an Ascent Hall550 Advance system, an X1 Advanced Diffraction System from Scintag Inc., a WYKO Optical Profiler Model 1100 system from Veeco, and a Nova Nano SEM 630 system from FEI, respectively.

RESULTS AND DISCUSSION

The single-layer intrinsic and Al-doped ZnO showed apparent difference from their combined bi-layer i/Al:ZnO in transmittance and reflectance spectra as seen in Fig. 1a. The Al:$Zn_{1-x}Mg_xO$ also showed variation in T% and R% spectra, being influenced by the content concentration (x = 0, 0.01, or 0.1) of MgO in the alloy, as seen in Fig. 1b. More detailed material information of the tested specimens is given in the upper half of Table 1, which includes type of TCO, MgO content, substrate temperatures during deposition, and film thickness if available. The initial and subsequent changes of sheet resistance (R_{sh}) from Hall measurements as a function of DH exposure time are given in the lower half. For the purpose of convenience to compare the degradation rate, as given in the bottom row, a linear degrading relationship was assumed. After 480 h DH exposure, all Al-doped ZnO films, including Al:$Zn_{1-x}Mg_xO$, became either insulating or highly resistive (> 1

$M\Omega$/square) and turned from initial clear to white hazy with visible delamination on some specimens. The calculations for the degradation rates in R_{sh} are therefore only up to 242 h for Al-doped ZnO, and 886 h for ITO and F-doped SnO_2. From the calculated degradation rates, it is clear that the ITO and F:SnO_2 were about two to four orders of magnitude more stable than ZnO-based films. For the
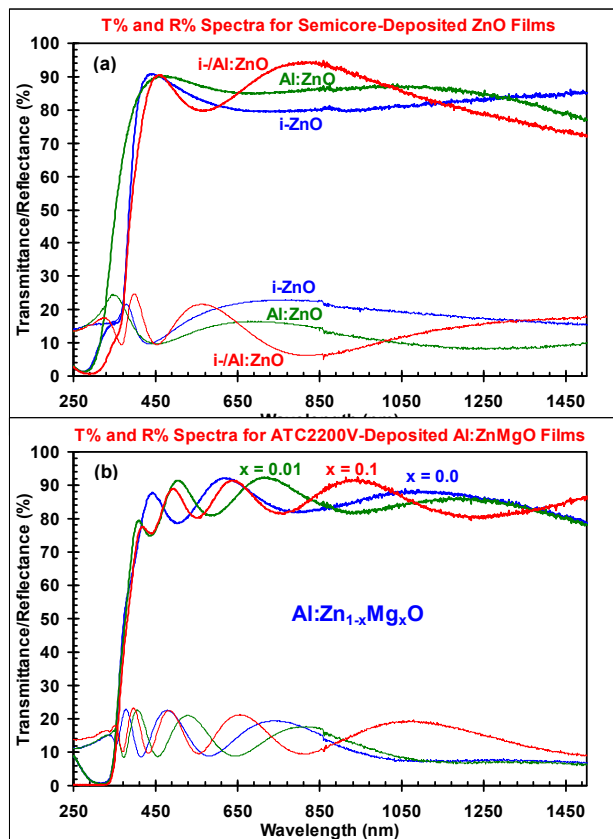

Fig. 1. Transmittance and reflectance spectra for (a) single-layer intrinsic, Al-doped, and intrinsic/Al-doped ZnO (i-ZnO, Al:ZnO, and i-/Al:ZnO), and (b) Al-doped $Zn_{1-x}Mg_xO$ films sputter-deposited on 1-mm-thick 7059 glass plates.

Table 1. Sample Data and Sheet Resistance Changes upon Damp Heat Exposure

Sample ID	IZO-11	AZO-21	BZO-31	AZO-383	AZO-471	AZO-501	AZO-681	AFL-1	L6A3-1	P-TCO1	P-TEC3
Composition	int.-ZnO	Al:ZnO	i-/Al:ZnO	Al:ZnO	Al:ZnO	Al:ZnO	Al:ZnO	Sn:In2O3	F:SnO2	F:SnO2	F:SnO2
MgO added	0%	0%	0%	0%	1%	10%	0%				
Dep. T_{sub} (^{o}C)	Ambient	Ambient	Ambient	Ambient	100	100	100	N/A	N/A	N/A	N/A
Thickness (µm)	0.1	0.1	0.2	0.3	0.5	0.5	0.6	N/A	0.5~0.6	0.26	N/A
DH Time (h)	**Rsh (ohm/sq)**										
0	HR*	85.71	64.03	68.19	73.30	HR*	29.34	83.00	8.30	17.92	12.53
120		967.00	107.70	155.60	165.50		39.11	77.87	7.98	17.15	12.82
242		15110.00	510.50	236.10	272.50		50.10	82.05	7.80	17.42	12.66
480		HR*	HR*	HR*	HR*		HR*	83.20	8.00	17.82	12.77
886	HR*: Highly resistive							84.34	8.24	17.38	12.69
Deg. Rate [(ohm/sq)/h]		6.21E+1	1.84E+0	6.94E-1	8.23E-1		8.58E-2	1.51E-3	-6.99E-5	-6.09E-4	1.80E-4

initially insulating intrinsic ZnO (ID# IZO-11) and 10%-MgO Al:Zn$_{0.9}$Mg$_{0.1}$O (ID# AZO-501), degradations were determined by measuring changes in optical properties, XRD, and micro-imaging. The results show that DH-induced R$_{sh}$ degradation rates of single- layer Al:ZnO films are faster for thinner films (e.g., AZO-21 vs. AZO-383). Also, Al:ZnO films deposited at ambient substrate temperature in the ATC system degraded faster than those deposited at 100°C substrate temperature (e.g., AZO-383 vs. AZO-681).
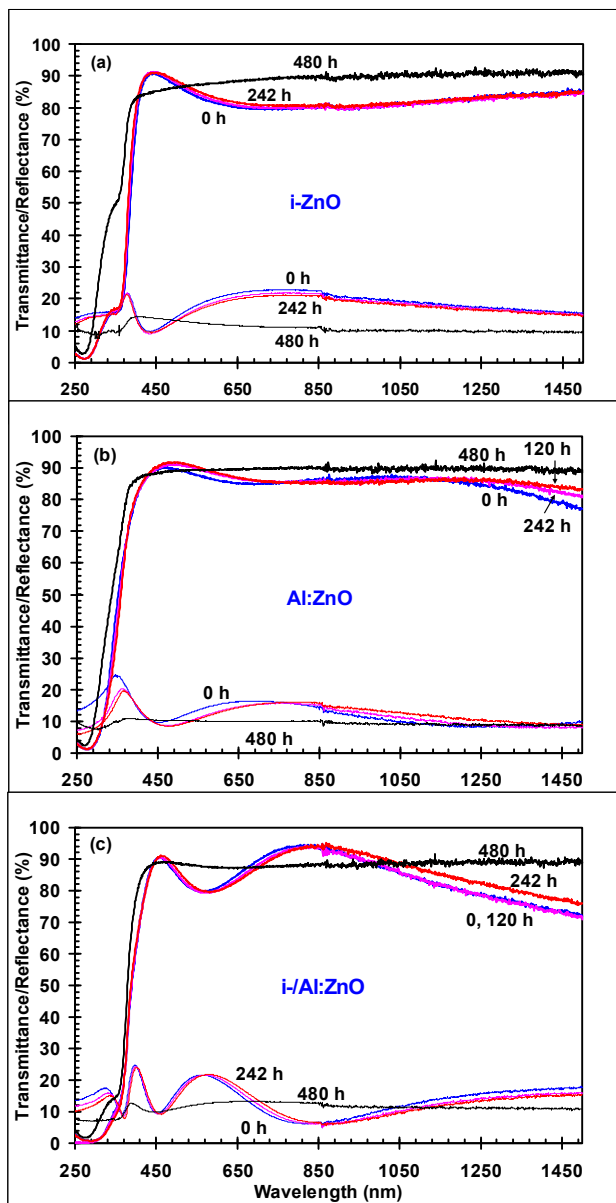
The single-layer i-ZnO, Al:ZnO, and their combined bi-layer i-/Al:ZnO did not show substantial changes in transmittance and reflectance spectra until after 480 h DH exposure, whereas the hazy films exhibited essentially the same flat curves losing the characteristic features of Al-doped conducting ZnO as shown in Fig. 2. This is also evidenced by the corresponding decrease in the mobility, determined by Hall measurements, as seen in Fig. 3a. One notable observation is that the degradation rate would be greater if the Al:ZnO specimens (not given in Table 1) were exposed in the DH chamber continuously for 240 h.

Fig. 2. Transmittance and reflectance spectra for (a) single-layer intrinsic ZnO (IZO-11), (b) single-layer Al-doped ZnO (AZO-21), and (c) bi-layer i/Al:ZnO (BZO-31) before (T0 = 0h) and after accumulating 120 h, 242 h, and 480 h DH exposure.
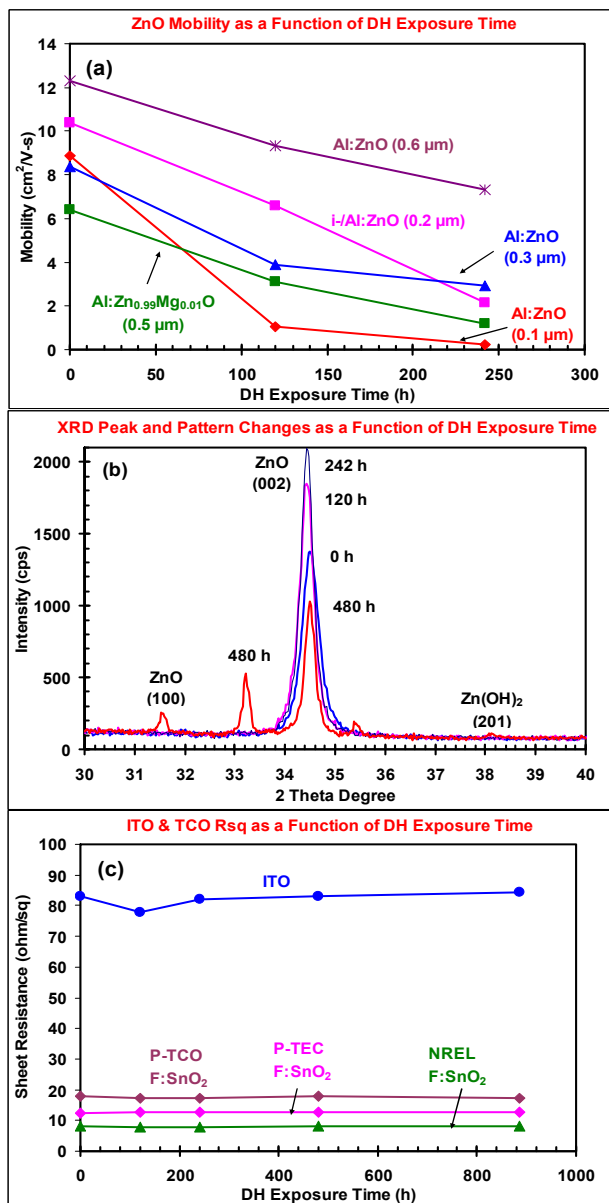

Fig. 3. (a) Decrease in mobility of mono- and bi-layer Al:doped ZnO films as a function of DH exposure time, (b) change in XRD feature for IZO-11 DH-exposed upto 480 h, and (c) sheet resistance of ITO and F:SnO$_2$ DH-exposed to 886 h.

3

The sample set would become insulating with a white hazy appearance, the same as those in Table 1 for 480 h with periodic removal from the DH chamber for measurements. This suggests that the films removed from the DH chamber were capable of recovering their physical properties to some extent, as also indicated by the gradual change to a somewhat less cloudy appearance after ~2 days in the air. One likely reason is the loss of water molecules from the hydrated or hydrolyzed film bulk and film/glass interface. Another interesting observation is that a bi-layer i-/Al:ZnO sample was highly resistive when it was still moist just after being taken out from a bottle filled with moisture in the DH chamber, and then became conducting as expected for a film with DH=94 h exposure after drying naturally in the air for some minutes. In comparison to the ZnO-based films, the optical property of the ITO and F:SnO$_2$ films were essentially unchanged in transmittance and reflectance spectra after 886 h DH exposure.

The structural changes by DH exposure are also reflected in the XRD patterns, per the example shown in Fig. 3b for the sample of intrinsic ZnO (IZO-11). Except for the bi-layer BZO-31, all single-layer ZnO films show an increase in (002) peak intensity at 34.50^{o} (2 theta) up to DH 242 h, possibly a result of morphological changes (see below), before exhibiting a moderate to large decrease at DH 480 h due to structural disintegration. For the Al:Zn$_{0.9}$Mg$_{0.1}$O (AZO-501) alloy, a main peak appeared at 34.12^{o} with a long tail. The main peak shifted to ~33.95^{o} upon DH exposure up to 242 h and then back to 34.12^{o} at 480 h. IZO-11 and AZO-471 were the two samples that produced four new peaks at DH 480 h (Fig. 3b), possibly a consequence of structural degeneration effected by the hot moisture-induced degradation. The peaks at 31.38^{o}, 33.22^{o}, and 35.38^{o} are assigned, using PDF#89-0510, 65-2880, and 75-1533 index references for ZnO, to be hexagonal (100), cubic (111), and hexagonal (101),

respectively. The peak at 38.12^{o} may be from cubic (200) or Zn(OH)$_2$ (201), as referred to PDF #65-2880 and 89-0138. Additionally, the peak width at half height for some samples showed notable narrowing at DH 480 h (e.g., Fig. 3b), but its cause is not yet clearly understood. These results suggest the ZnO might have undergone structural degeneration from original highly (002) preferential orientation to a more disordered state with some transformation from original hexagonal to cubic, in addition to the formation of insulating ZnO and Zn(OH)$_2$. Meanwhile, it is not clear yet on the fate of the Al dopant upon DH exposure, although it is possible that the Al was also readily transformed into Al(OH)$_3$.

The surface morphology of the various TCO films was also examined periodically for the initiation and propagation of the defecting patterns and regions as a function of DH exposure time by using the WYKO interference optical microscope. More than 1000 micro-images were taken. A few of the images are illustrated in Fig. 4 for the IZO-11sample at four stages, showing the progressive morphological degradation as the DH exposure time increased to 480 h. The initially grainy but fairly smooth surface started to show some small spikes that appeared in a random manner upon exposure to DH in the first ~100 h. The number of spikes increased along with the appearance of full or partial ring-like features that showed ditch-like cutting into the depth of the film as the DH time increased (e.g., 240 h). The ring features are suspected to arise from the finite water droplets condensed from the moisture, which was the case observed when the cool films were just loaded into the hot steamy DH chamber. As the degradation progressed further, the film disintegrated greatly into fabrics-like features at DH 480 h and was difficult to be micro-photographed because of large loss of light reflection from the rough surface. This morphological degradation process and pattern development was essentially the
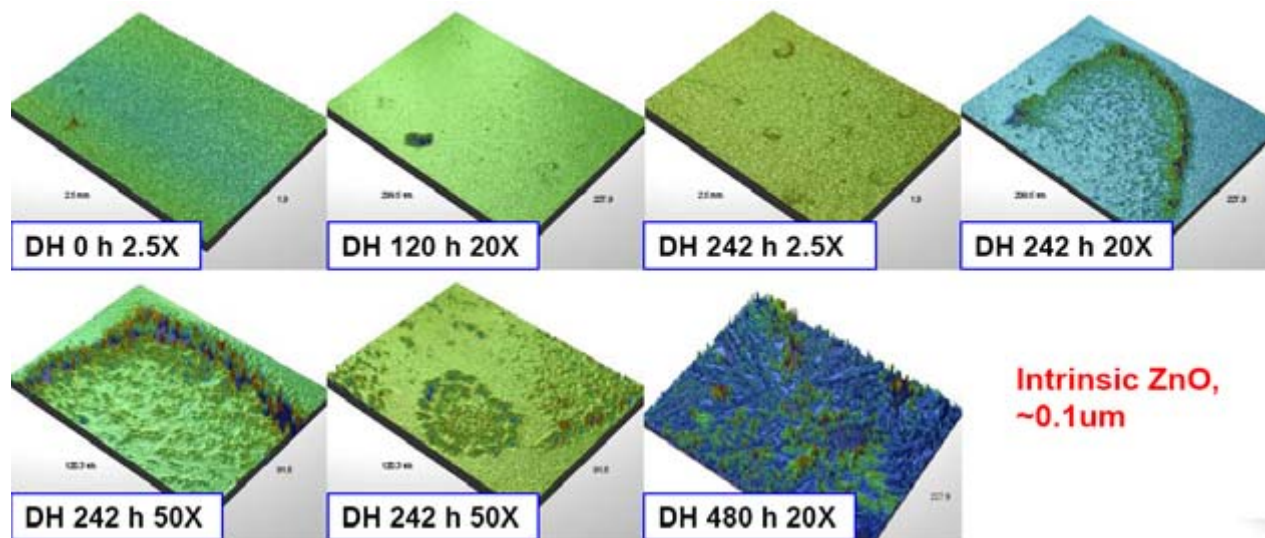

Fig. 4. Optical micro-images for the sample of intrinsic ZnO (IZO-11), showing the progressive morphological degradation as the DH exposure time increased to 480 h. The magnification factors are also indicated.

same for all ZnO-based films as observed in this study. While starting with grainy surfaces for the Semicore-deposited Al:ZnO, the DH exposure at 480 h resulted in obvious morphological differences for the single-layer i-ZnO and Al:ZnO, and bi-layer i-/Al:ZnO, as shown by SEM topographs in Fig. 5. Similar surface morphological degradations for the two samples of Al:Zn$_{1-x}$Mg$_x$O alloy (top row), ITO and the experimental P-TCO F:SnO$_2$ (bottom row) at DH 242 h are illustrated in Fig. 6. The T-PEC F:SnO$_2$ also exhibited a similar pattern of changes as ITO and P-TCO (not shown). At 10% of MgO, the Al:Zn$_{0.9}$Mg$_{0.1}$O (AZO-501) was originally insulating and, upon DH exposure, exhibited localized spot-wise material loss (see the third image on the top row of Fig. 6), suggesting the MgO-ZnO was not fully alloyed during co-sputtered process.

In comparison with Al-doped ZnO and Zn$_{1-x}$Mg$_x$O alloy, the ITO and F:SnO$_2$ were more stable with little or no changes in the overall optical and structural properties upon 886 h DH exposure (figures not shown), although optical micro-images revealed finite corrosions occurring at DH 242 h (Fig. 6, bottom row). All three F:SnO$_2$ samples tested were definitely more stable than the ITO at 886-h DH exposure. Although the low degradation rates and relatively flat curves for sheet resistance, R$_{sh}$, of ITO and F:SnO$_2$, as seen in Table 1 and Fig. 3c, up to DH 886 h may suggest their high stability against the damp heat, the truth is that the R$_{sh}$ values at DH 480 h and 886 h were obtained by moving the four contact probes in the Hall measurements around the film surfaces to avoid the highly resistive regions or spots as illustrated in Fig. 6 (bottom row). This was especially required for the ITO sample (AFL-1) at DH 886 h having a number of large and small highly resistive regions or spots. The measured R$_{sh}$ values

are therefore for the surface areas that still possessed continuous conducting paths. Overall, when compared with ZnO and ITO, F:SnO$_2$ films were more stable, as could be expected also from the literature [6]. Among all three, the NREL F:SnO$_2$ (L6A3-1) showed the highest stability in all aspects against damp heat even with very little change in optical morphological micro-imaging observations.

Regardless of the film composition and the obvious difference in the degradation rate, the degradation behavior appears similar for all TCO films studied, as
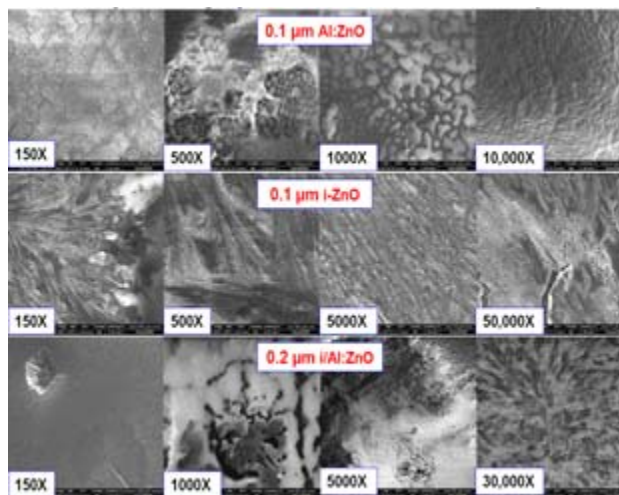

Fig. 5. SEM topographical microimages for the samples of Al:ZnO (AZO-21), i-ZnO (IZO-11), and bilayer i-/Al:ZnO (BZO-31) at DH exposure of 480 h. The magnification factors are also indicated.
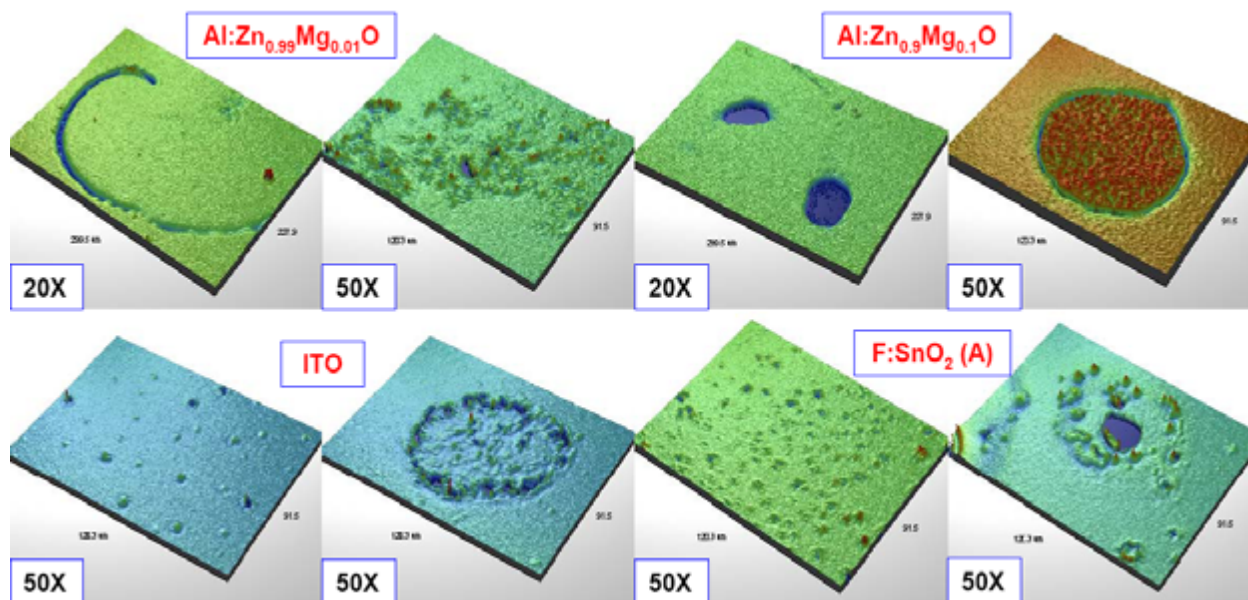

Fig. 6. Optical micro-images for the samples of (top row) Al:Zn$_{1-x}$Mg$_x$O (x = 0.01 and 0.1); and (bottom row) ITO, and P-TCO F:SnO$_2$, showing morphological degradations at DH 242 h exposure. The magnification factors are also indicated.

inferred from optical micro-imaging observations. In general, the first sign of degradation started at a few small spots or areas with appearance of irregular circles and spikes (e.g., Figs. 4 and 6 at 120~242 h); as the DH exposure increased, the hydrolysis-induced corrosion circles, spikes, and pop-ups increased and became more widely spread (e.g., Figs. 4 and 6 at DH 242 h), and finally, especially for ZnO-based films, severe disintegration resulted (e.g., Fig. 4 at DH 480 h). This thermal hydrolytic process might have started from the surface of the film as well as at the grain boundary and progressed downward and inward. If this was the case, then it would take longer exposure time to allow the "ditches" (e.g., Fig. 4, leftmost figure at the bottom row) to grow deeper to break up the electrical conducting path on a thicker ZnO film, and to break up the better grain crystallites on a ZnO film made at higher temperature. In addition, visible delaminations were seen on some ZnO films after 480 h DH exposure, suggesting the destruction of the bonding at the interface between the ZnO layer and glass substrate. On the other hand, with extended DH exposure to 886 h, the ITO (AFL-1) film showed two large and some small insulating regions, while $F:SnO_2$ films remained *visibly* intact. Accordingly, based on all the optical, electrical, structural and morphological observations, the temporal process of DH-induced degradation is proposed to involve first hydrolysis of the oxides at some sporadic "weak" spots, swelling and popping of the hydrolyzed spots due to volume increase, "segregation" of hydrolyzed regions causing discontinuity of electrical path, hydrolysis of the oxide-glass interface, and finally formation of insulating $M(OH)_2$ along with visible delamination over larger areas.

CONCLUSIONS

We have shown the relative stability of a number of TCOs, including intrinsic and Al-doped ZnO, Al-doped $Zn_{1-x}Mg_xO$, ITO, and F-doped SnO_2, on glass substrates when exposed to damp heat at 85^oC and 85% RH. From the electrical, optical, structural, and morphological analysis, the order of degradation rate is determined to be ZnO >> ITO > $F:SnO_2$. With only one conducting Al-doped $Zn_{1-x}Mg_xO$ alloy at x = 1% that failed in the DH test in the same way as other Al:ZnO samples, it is too premature to conclude whether the alloy has the potential with appreciable stability to replace Al:ZnO. New experiments will be conducted to examine the stability of single-layer i-ZnO and Al:ZnO, bilayer i-/Al:ZnO, and interconnect contact resistance of bilayer i-/Al:ZnO on Mo as a function of temperature and relative humidity in order to determine the activation energy of degradation. The protective effectiveness of moisture-blocking SiO_xN_y barrier coating deposited by PECVD process coupled with surface chemical treatment using PDMS silane [1] and DH-resistant SnO_2 on bi-layer i-/Al:ZnO will be also investigated.

REFERENCES

1. J. Pern and R. Noufi, " An Investigation of Stability Issues of ZnO and Mo on Glass Substrates for CIGS Solar Cells upon Accelerated Weathering and Damp Heat Exposures," DOE SETP Review Meeting, Denver, CO., April 17-19, 2007. http://www1.eere.energy.gov/solar/review_meeting/pdfs/p_9_pern_nrel.pdf.

2. A.W. Czanderna and F.J. Pern, "Encapsulation of PV Modules using Ethylene Vinyl Acetate Copolymer as A Pottant: A Critical Review," *Solar Energy Materials and Solar Cells*, **43** (1996) 101-181.

3. M. Bär, J. Reichardt, I. Sieber, A. Grimm, I. Kötschau, I. Lauermann, S. Sokoll, T.P. Niesen, M.C. Lux-Steiner, and Ch.-H. Fischer, "ZnO Layers Deposited by the Ion Layer Gas Reaction on $Cu(In, Ga)(S, Se)_2$ Thin Film Solar Cell Absorbers – Impact of 'Damp Heat' Conditions on the Layer Properties," *Progr. Photovolt: Res. Appl.* **15** (2007) 187–198.

4. J. Klaer, R. Klenk, A. Boden, A. Neisser, C. Kaufmann, R. Scheer, H.-W. Schock, "Damp Heat Stability of Chalcopyrite Mini-Modules: Evaluation of Specific Test Structures," *Proc. 31st IEEE PVSC*, (2005) 336-339.

5. H. Stiebig, W. Reetz, C. Haase, T. Rapmann, and B. Rech, "Stability of Non-encapsulated Thin-Film Silicon Solar Cells in Damp Heat Tests," *Proc. 15th International PV Sci. & Eng. Conf. (PVSEC-15)*, Shanghai, China, 2005, 561-562.

6. R. G. Gordon, "Criteria for Choosing Transparent Conductors," *MRS Bulletin*, **25** (2000), 52-57.

REPORT DOCUMENTATION PAGE

1. REPORT DATE (DD-MM-YYYY)	2. REPORT TYPE	3. DATES COVERED (From - To)
May 2008	Conference Paper	11-16 May 2008

4. TITLE AND SUBTITLE
Damp-Heat Induced Degradation of Transparent Conducting Oxides for Thin-Film Solar Cells: Preprint

5a. CONTRACT NUMBER
DE-AC36-99-GO10337

5b. GRANT NUMBER

5c. PROGRAM ELEMENT NUMBER

6. AUTHOR(S)
J. Pern, R. Noufi, X. Li, C. DeHart, and B. To

5d. PROJECT NUMBER
NREL/CP-520-42525

5e. TASK NUMBER
PVB76701

5f. WORK UNIT NUMBER

7. PERFORMING ORGANIZATION NAME(S) AND ADDRESS(ES)
National Renewable Energy Laboratory
1617 Cole Blvd.
Golden, CO 80401-3393

8. PERFORMING ORGANIZATION REPORT NUMBER
NREL/CP-520-42525

9. SPONSORING/MONITORING AGENCY NAME(S) AND ADDRESS(ES)

10. SPONSOR/MONITOR'S ACRONYM(S)
NREL

11. SPONSORING/MONITORING AGENCY REPORT NUMBER

12. DISTRIBUTION AVAILABILITY STATEMENT
National Technical Information Service
U.S. Department of Commerce
5285 Port Royal Road
Springfield, VA 22161

13. SUPPLEMENTARY NOTES

14. ABSTRACT (Maximum 200 Words)
The stability of intrinsic and Al-doped single- and bi-layer ZnO for thin-film CuInGaSe2 solar cells, along with Al-doped Zn1-xMgxO alloy and Sn-doped In2O3 (ITO) and F-doped SnO2, was evaluated by direct exposure to damp heat (DH) at 85oC and 85% relative humidity. The results show that the DH-induced degradation rates followed the order of Al-doped ZnO and Zn1-xMgxO >> ITO > F:SnO2. The degradation rates of Al:ZnO were slower for films of higher thickness, higher substrate temperature in sputter-deposition, and with dry-out intervals. As inferred from the optical micro-imaging showing the initiation and propagation of degrading patterns and regions, the degradation behavior appears similar for all TCOs, despite the obvious difference in the degradation rate. A degradation mechanism is proposed to explain the temporal process involving thermal hydrolysis.

15. SUBJECT TERMS
CIGS; PV; transparent conducting oxide; damp- heat induced degradation; sputter deposition; thin film; optical micro-imaging; thermal hydrolysis;

16. SECURITY CLASSIFICATION OF:			17. LIMITATION OF ABSTRACT	18. NUMBER OF PAGES	19a. NAME OF RESPONSIBLE PERSON
a. REPORT	b. ABSTRACT	c. THIS PAGE	UL		
Unclassified	Unclassified	Unclassified			19b. TELEPHONE NUMBER (Include area code)